Residual Stresses in Ti-6Al-4V Parts Manufactured by Direct Metal Laser Sintering and Electron Beam Melting

G. Lim[1a], K. Lau[1], W.S. Cheng[1], Z. Chiang[1], M. Krishnan[1] and D. T. Ardi[1]

[1]Advanced Remanufacturing and Technology Centre (ARTC), No. 3, Cleantech Loop, #01-01, CleanTech Two, Singapore 637143

[a]limgw@artc.a-star.edu.sg

Introduction

Direct Metal Laser Sintering (DMLS) and Electron Beam Melting (EBM) are two unique powder bed Additive Manufacturing (AM) processes that allow the fabrication of customized, complex and functional metallic parts by consolidating layers of powder via melting with intense energy sources. The high input of beam energy leads to adverse thermal gradients which can induce undesirable residual stresses in the AM parts. However, EBM process involves pre-heating and slow cooling stages that allow the production of parts with lower residual stresses. In recent years, both of these processes have experienced a surge in their demand due to the benefits of producing high value added components with complex geometry at lower cost and shorter lead time as compared to conventional manufacturing processes. However, the current lack of documentation in the overall reliability of AM parts is withholding the widespread usage in various industries [1]. Knowledge in the nature of residual stresses in AM processes is crucial in tackling compelling residual stress related problems such as warpage, cracking, delamination and performance deficit.

Objective

This paper presents a review of work carried out to characterize the residual stresses in DMLS and EBM Ti-6Al-4V specimens using centre-hole drilling (CHD), X-ray diffraction (XRD) and Contour Method (CM).

Methodology

Specimen fabrication. DMLS Ti-6Al-4V specimens were fabricated using EOS M290 machine and EBM Ti-6Al-4V specimens were fabricated using ARCAM A2XX equipment. The Ti-6Al-4V specimens were produced using Ti-6Al-4V powders supplied by EOS and ARCAM respectively. Default printing strategies were used to fabricate the coupons. DMLS and EBM specimens were built on Ti-6Al-4V and stainless steel baseplates respectively. The equipment specifications are summarized in Table 1.

Parameter	DMLS	EBM
Energy source	Yb-fibre laser	Electron beam
Max. scan speed	7000 mm/s	8000 mm/s
Max. beam power	400 W	3000 W
Beam spot size	80 µm	0.2 – 1.0 mm (cont. variable)

Table 1 Process Parameters for DMLS and EBM

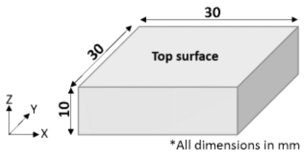

Fig. 1 Specimen geometries

All the specimens possessed the same nominal dimensions: 30 x 30 x 10 mm (L x W x H). The specimen build direction is along the z-axis, see Fig. 1. DMLS specimens were divided into two groups: heat-treated and non-heat treated. The purpose of carrying out heat treatment is to relieve the residual stress accumulated in the parts during DMLS process. For heat-treated specimens, the specimens were heat-treated after removing from EOS M290 in a argon gas atmosphere at 650˚C for 3 hours. The specimens were then removed from the baseplate via wire electrical discharge machining (WEDM). For non-heat treated specimens, the specimens were removed from baseplate via WEDM directly after printing in EOS M290. EBM specimens were removed from their baseplate manually after fabrication.

Residual stress. All the residual stress measurement techniques were performed using Poisson’s ratio and Young’s modulus at 0.32 and 115 GPa respectively. Residual stresses in the longitudinal direction (x-axis) and transverse direction (y-axis) from the centre of the top surface of the specimens to 1 mm depth were assessed using CHD and XRD. CHD residual stress measurements were carried out using SINT Technology Restan MTS-3000 with HBM K-RY61-1.5/120R Type-B strain gauge rosettes in accordance to ASTM E837-13 non-uniform stress analysis. XRD residual stress measurements were performed using Stresstech Xstress 3000 G3/G3R with Cu X-ray source, Ni K-β filter and 4 mm collimator. The analyses were done using modified-χ measurement mode with $\sin^2\Psi$ method. Chemical etching using hydrofluoric acid was done to remove material for XRD to perform sub-surface residual stress measurements. CM residual stress determination was performed by first sectioning the specimens in equal halves along the y-axis using WEDM. Subsequently, the sectioned surfaces were scanned using Alicona Infinite Focus G4 to assess the surface contours. The data was then processed in MATLAB and transferred to Siemens NX Advanced Simulation to produce 2D residual stress maps. None of residual stress measurement techniques were performed on the same specimen in any given circumstances.

Experimental Findings

Residual stress measurement results for DMLS non-heat treated, DMLS heat treated and EBM specimens are presented in Fig. 2 and Fig. 3. CHD measurements were not performed on DMLS heat treated specimens. CM residual stress data were extracted along the centre axis of the 2D residual stress maps shown in Fig. 4 from 0.5 mm to 9.5 mm depth. DMLS non-heat treated specimens displayed non-equibiaxial compressive residual stresses in the near-surface region. The residual stresses then became more tensile in the subsequent depths. DMLS heat treated specimens displayed equibiaxial surface tensile residual stresses while EBM specimens displayed highly equibiaxial compressive residual stresses on the surface. For both latter cases, the stresses become negligible in the subsequent depths.

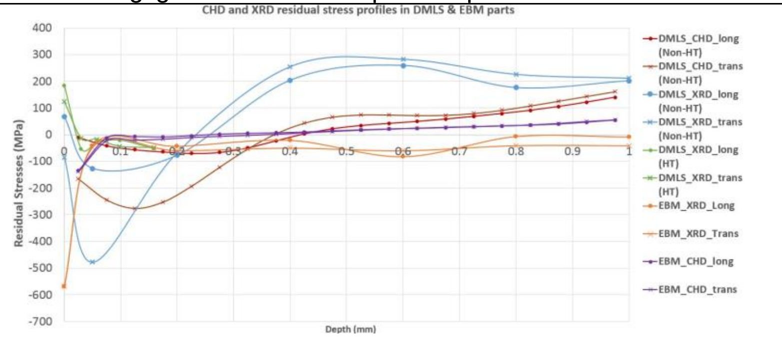

Fig. 2 Surface and near-surface residual stresses

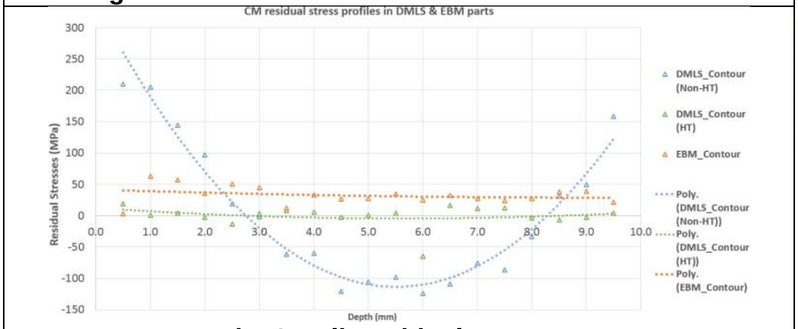

Fig. 3 Bulk residual stresses

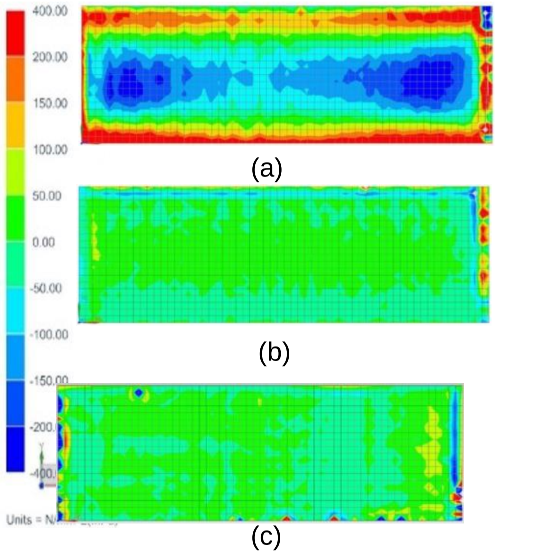

Fig. 4 Contour residual stress map for (a) DMLS non-heat treated (b) DMLS heat treated and (c) EBM specimens

DMLS non-heat treated specimens possessed an interesting compressive residual stress distribution in the region beneath the top surface. This is contradictory to consensus in many literature that residual stresses in the top region should be tensile [2,3,4,5]. However, compressive residual stresses in the top region were also reported in a few literature [6,7] and are attributed to martensitic transformation. The compressive residual stress distribution shares some similarities with the typical shot peening induced residual stress profile on conventional material. This finding suggests potential future work on the engineering of the required residual stresses during the AM built process. Residual stresses measured on DMLS heat treated specimens indicate the stress-relieving effects of the heat treatment process. EBM residual stress profiles justify the stress reduction benefits of the pre-heating and slow cooling stages.

Conclusion

Residual stresses in the DMLS and EBM specimens were determined using CHD, XRD and CM techniques. CHD and XRD residual stress measurement results of DMLS non-heat treated specimens did not show good agreement. This highlights the challenge in assessing the as-built AM specimens which usually contains non-isotropic structures and properties. The determination of the measurement discrepancies between CHD and XRD, nature of the compressive residual stresses and their impact on part quality will be studied in the future.

References

[1] S. Daniewicz and N. Shamsaei, "An introduction to the fatigue and fracture behaviour of additive manufactured parts," *International Journal of Fatigue,* vol. 94, no. 2, p. 167, 2017.

[2] I. van Zyl, I. Yadroitsava and I. Yadroitsev, "Residual stress in Ti6Al4V objects produced by direct metal laser sintering," *South African Journal of Industrial Engineering,* vol. 27, no. 4, pp. 134-141, 2016.

[3] P. Mercelis and J.-P. Kruth, "Residual stresses in selective laser sintering and selective laser melting," University of Leuven, Leuven, 2006.

[4] M. F. Zaeh and G. Branner, "Investigations on residual stresses and deformations in selective laser melting," Springer Berlin Heidelberg, Berlin, 2010.

[5] B. Vrancken, "Study of residual stresses in selective laser melting," Arenberg Doctoral School, Arenberg, 2016.

[6] B. Vracken, R. Wauthle, J.-P. Kruth and J. Van Humbeeck, "Study of the influence of material properties on residual stress in selective laser melting," in *Solid Freeform Fabrication Symposium*, Texas, 2013.

[7] S. Ghosh and J. Choi, "Deposition pattern based thermal stresses in single-layer laser aided direct material deposition process," *Journal of Manufacturing Science and Engineering,* vol. 129, no. 2, pp. 319-332, 2007.